Mechanism of superexchange interatomic Coulombic decay in rare-gas clusters

Petra Votavová,[1] Tsveta Miteva,[2] Selma Engin,[2] Sévan Kazandjian,[2] Přemysl Kolorenč,[1] and Nicolas Sisourat[2,*]

[1]*Charles University, Faculty of Mathematics and Physics, Institute of Theoretical Physics, V Holešovičkách 2, 180 00 Prague, Czech Republic*

[2]*Sorbonne Université, CNRS, Laboratoire de Chimie Physique – Matière et Rayonnement, F-75005 Paris, France*

(Received 17 July 2019; published 23 August 2019)

Interatomic Coulombic decay (ICD) is an ultrafast energy transfer process. Via ICD, an excited atom can transfer its excess energy to a neighboring atom which is thus ionized. On the example of the NeHeNe cluster, we recently reported [Phys. Rev. Lett. **119**, 083403 (2017)] that the total ICD widths are substantially enhanced in the presence of an ICD inactive atom. The enhancement occurs due to the coupling of the resonance state to intermediate virtual states of the bridge atom—a mechanism named superexchange ICD. In this followup work, we analyze the partial ICD widths in the NeHeNe cluster and show that only some channels are affected by the superexchange ICD process. Furthermore, we consider superexchange ICD in NeHeAr. We show that in this system the enhancement is still present but the energy transfer mediated by the superexchange mechanism is less efficient than in NeHeNe owing to the different ionization potentials of Ar and Ne. The behavior of the computed ICD widths is explained with a simple model based on first-order perturbation theory and a Hartree-Fock-like description of the states.

DOI: 10.1103/PhysRevA.100.022706

I. INTRODUCTION

Interatomic Coulombic decay (ICD) is an ultrafast energy transfer process between two weakly bound systems [1–3]. In ICD, an excited *donor* partner has enough excess energy to ionize an *acceptor* one. The most typical example is that of a neon dimer after 2*s* ionization of one neon atom within the dimer. This excited neon ion is the donor atom and relaxes within 150 fs [4,5] by transferring its excess energy to the neutral neighboring neon atom (i.e., the acceptor), which is thus ionized.

ICD is a general effect which has been observed in many diverse situations [6–9]. Its mechanism has been discussed in [10]. In the latter reference, the authors showed that when the donor-acceptor distance R is large the energy transfer can be pictured as an exchange of a virtual photon: the donor emits a virtual photon which is absorbed by the acceptor. In such a case, the ICD rates behave as R^{-6}. At shorter interatomic distances, the orbitals of the donor and acceptor systems overlap and the ICD rates are much larger than predicted by the virtual photon mechanism.

Recently, we have shown that another mechanism is possible when the donor and acceptor systems are separated by a bridge atom. On the example of the neon-helium-neon trimer, we have shown that ICD between the two neon atoms after 2*s* ionization of one neon atom exhibits total widths that are substantially enhanced in the presence of a helium atom compared to the isolated neon dimer [11]. Furthermore, we have shown that this mechanism, so-called superexchange ICD, is mediated by the presence of energetically close intermediate configurations. Note also that a virtual photon approximation was recently derived for three-body ICD processes [12].

In the following, we analyze both the total and partial ICD widths of neon-helium-neon and neon-helium-argon trimers. It is shown that, owing to symmetry reasons, only particular channels are enhanced by the superexchange mechanism. We also demonstrate that, because of the difference in ionization potential between neon and argon, the superexchange contribution is significantly reduced in the neon-helium-argon system compared to the neon-helium-neon trimer. Furthermore, we present in detail a model based on first-order perturbation theory which provides insights into the superexchange mechanism.

The outline of the article is the following. In Sec. II, we describe the theoretical methods and computational details employed to calculate the total and partial ICD widths. Furthermore, a model based on first-order perturbation theory, which helps the interpretation of the *ab initio* results, is detailed. In Sec. III we present and discuss the results for the neon-helium-neon and neon-helium-argon trimers. The article ends with the conclusions of this work. Atomic units are used throughout unless stated otherwise.

II. METHODS AND COMPUTATIONAL DETAILS

A. Fano-configuration interaction method

We employed the Fano-configuration interaction (Fano-CI) method [13] to compute the total and partial widths of neon-helium-neon and neon-helium-argon trimer after 2*s* ionization of one neon atom. The method was presented in detail in [13]; here we outline it briefly.

In Fano theory [14,15], a resonance is described as a discrete state Φ, embedded in and coupled to one or several continua. The ICD widths are then given by the coupling

*nicolas.sisourat@sorbonne-universite.fr

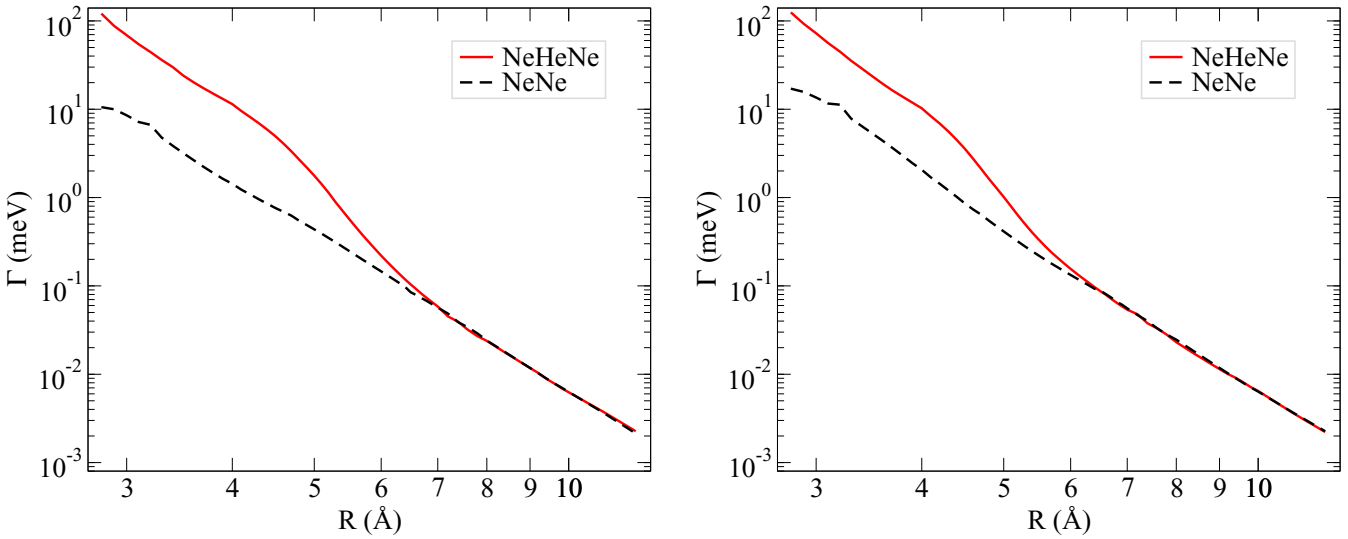

FIG. 1. Comparison between the total decay widths of the $Ne^+(2s^{-1})\,^2\Sigma^+_{g,u}$ states in Ne_2 (black dashed lines) and NeHeNe (red full lines). Left panel: $Ne^+(2s^{-1})\,^2\Sigma^+_g$. Right panel: $Ne^+(2s^{-1})\,^2\Sigma^+_u$.

between the discrete state and the continuum states $|\chi_{\beta,\epsilon_\beta}\rangle$

$$\Gamma = \sum_\beta \Gamma_\beta = 2\pi \sum_\beta |\langle\Phi|\hat{H} - E_r|\chi_{\beta,\epsilon_\beta}\rangle|^2, \tag{1}$$

where Γ is the total width and Γ_β the partial width corresponding to the decay channel β. The kinetic energy of the ICD electron for a given channel β is ϵ_β and E_r is the energy of the inner-valence ionized state. We use a simple CI scheme to describe both parts: the discrete part is a one-hole (1h) configuration where an electron is removed from an inner-valence orbital of the Hartree-Fock (HF) determinant of the neutral system. The continuum part is obtained by performing CI calculations where the ICD electron is approximated by the Hartree-Fock virtual orbitals. A CI calculation is performed for each virtual orbital separately, which leads to small sized matrices to be diagonalized. Since the virtual orbitals do not have the proper boundary conditions, a Stieltjes imaging technique is employed to recover the correct widths from the approximated ones [16–18]. Similar to Ref. [19], we computed the decay width as the average over a range of Stieltjes orders, for which it does not vary substantially.

We used restricted Hartree-Fock molecular orbitals optimized for each system. The aug-cc-pVTZ basis set [20] augmented with $[7s, 7p, 7d]$ diffuse functions of the Kaufmann-Baumeister-Jungen (KBJ) type [21] functions was employed on all atoms in the case of the NeHeNe trimer and NeNe dimer. The aug-cc-pVQZ basis set [20] augmented with $[6s, 6p, 6d]$ KBJ functions was used in the case of NeHeAr and NeAr. In order to compute the ICD widths for the trimers and dimers with the same basis sets, a ghost atom X was placed at the position of He for the NeNe and NeAr calculations. Additionally, $[3s, 10p, 3d]$ diffuse KBJ functions were added at the midpoints between Ne-He and He-Ar in the case of NeHeAr and Ne-X and X-Ar in the case of NeXAr. A larger basis set for NeAr and NeHeAr was thus employed in order to ensure convergence of the results. We attribute the need for a larger basis set for these systems to the higher ICD electron energy.

Within the framework of the Fano-CI method, the partial width Γ_β to a given decay channel can be expressed as

$$\Gamma_\beta = 2\pi \left|\langle\Phi|\hat{H} - E_r|\Phi^{2h}_\beta k_\beta\rangle\right|^2, \tag{2}$$

where we represent the decay channel as a product of a doubly ionized CI state Φ^{2h}_β and an electron excited to a virtual orbital k. To calculate these quantities, we assume that the pseudocontinuum final states $\tilde{\chi}^a_q$ computed using the Fano-CI method form a complete basis. We expand the $\Phi^{2h}_\beta k_\beta$ wave function in this basis

$$\Gamma_\beta = 2\pi \left| \sum_{aq} \langle\Phi|\hat{H} - E_r|\tilde{\chi}^a_q\rangle\langle\tilde{\chi}^a_q|\Phi^{2h}_\beta k_\beta\rangle \right|^2. \tag{3}$$

Each Fano-CI state $\tilde{\chi}^a_q$ is represented as a linear combination of $2h1p$ configurations (singly ionized excited Slater determinants); we can thus rewrite the above equation as

$$\Gamma_\beta = 2\pi \left| \sum_{aq} (\mathbf{T}\mathbf{d}^a)_{\beta q} \langle\Phi|\hat{H} - E_r|\tilde{\chi}^a_q\rangle \right|^2, \tag{4}$$

where $\mathbf{T}$ is the matrix obtained after diagonalization of the matrix of $2h$ configurations and $\mathbf{d}^a$ is the matrix of expansion coefficients of the Fano-CI states. The matrix elements $\langle\Phi|\hat{H} - E_r|\tilde{\chi}^a_q\rangle$ are easily evaluated as sums of two-electron integrals and HF orbital energies [13].

B. First-order perturbation theory based model

In [11], we have shown that the superexchange ICD mechanism in NeHeNe is mediated by $Ne^+He^-Ne^+$ virtual states. In that case, we have derived an approximate expression for the ICD widths as a function of the NeNe internuclear distance. In order to interpret the results from the Fano-CI calculations we employ the same model here. A more detailed derivation is however given. Furthermore, we use the symmetries of

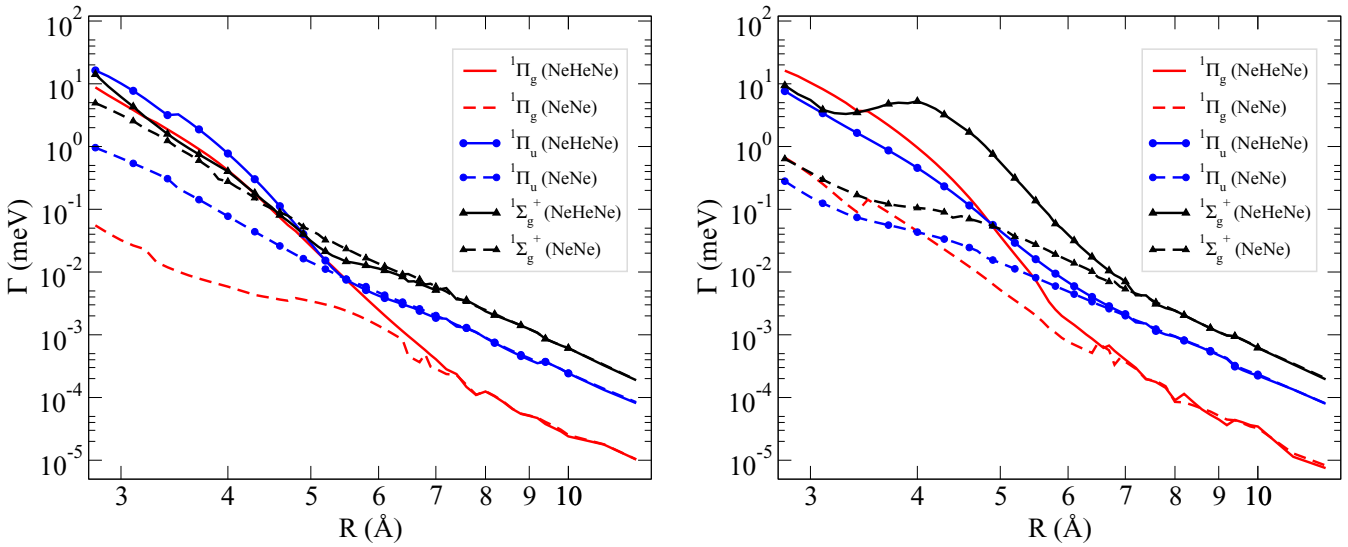

FIG. 2. Comparison between the partial decay widths of the $Ne^+(2s^{-1})\,^2\Sigma^+_{g,u}$ states in Ne_2 (dashed lines) and NeHeNe (full lines) to *singlet* final states. We show only the channels whose decay widths are enhanced as a result of the superexchange ICD: $^1\Pi_g$, $^1\Pi_u$, and $^1\Sigma_g^+$. Left panel: $Ne^+(2s^{-1})\,^2\Sigma^+_g$. Right panel: $Ne^+(2s^{-1})\,^2\Sigma^+_u$.

the system to analyze the partial ICD widths. We start from Eq. (1) for a given channel β

$$\Gamma_\beta = 2\pi|\langle\Phi|\hat{H} - E_r|\chi_{\beta,\epsilon_\beta}\rangle|^2. \tag{5}$$

Using first-order perturbation theory and a single configuration state function (CSF) for each state, we have

$$|\Phi\rangle = c_i|\Psi_0\rangle \tag{6}$$

and

$$|\chi_{\beta,\epsilon_\beta}\rangle = c_a^\dagger c_j c_k|\Psi_0\rangle + \sum_J \frac{H^\beta_{Jf}}{E^\beta_f - E_J} c_J^\dagger c_j c_k|\Psi_0\rangle, \tag{7}$$

where i, j, and k are occupied orbitals of the donor and acceptor systems defining the channel β, a represents a continuum orbital, and J is a virtual orbital of the bridge atom. The creation and annihilation operators are denoted as $c^\dagger$ and c, respectively. In the above equation, H_{Jf} is the Hamiltonian matrix element between the $c_a^\dagger c_j c_k|\Psi_0\rangle$ and $c_J^\dagger c_j c_k|\Psi_0\rangle$ CSFs, where $|\Psi_0\rangle$ denotes the Hartree-Fock ground state. The energy expectation values of these two CSFs are E^β_f and E_J, respectively.

Including Eqs. (6) and (7) into Eq. (5), we obtain

$$\langle\Phi|\hat{H} - E_r|\chi_{\beta,\epsilon_\beta}\rangle = \sqrt{\frac{3}{2}}\left(\langle ai|jk\rangle - \langle ai|kj\rangle + \sum_J \frac{H^\beta_{Jf}}{E^\beta_f - E_J}(\langle Ji|jk\rangle - \langle Ji|kj\rangle)\right). \tag{8}$$

In the above expression, we assume that the final state β is a triplet state. Similar derivation is easily done for a singlet state [13]. The first two terms on the right-hand side (RHS) of Eq. (8) correspond to the direct ICD process (the first term is the direct term and the second the exchange one as in [22]). The terms in the sum over J are the ones corresponding to the superexchange mechanism. In what follows, we focus on the range of distances where these terms dominate over the direct ICD ones (e.g., $R < 6$–7 Å for a linear NeHeNe trimer; see [11] and below). Furthermore, we assume that (i) the donor and acceptor orbitals form an orthogonal basis set and (ii) the donor and acceptor orbitals are *not* orthogonal to those of the bridge atom. We then expand the Coulomb operator as in [22]. In the particular case of a linear geometry and keeping only the dominant terms, Eq. (8) then reads

$$\langle\Phi|\hat{H} - E_r|\chi_{\beta,\epsilon_\beta}\rangle = \sqrt{\frac{3}{2}}\sum_J \frac{H^\beta_{Jf}}{R^2\left(E^\beta_f - E_J\right)}(\langle J|j\rangle\langle i|z|k\rangle - \langle J|k\rangle\langle i|z|j\rangle). \tag{9}$$

As defined above, R is the distance between the donor and acceptor species (i.e., Ne-Ne and Ne-Ar below). Several observations can be made at this point. First, contrary to the direct ICD mechanism whose rates are proportional to R^{-6}, the superexchange terms exhibit an R^{-4} behavior. Note, however, that the terms $\langle J|k\rangle$ and $\langle J|j\rangle$ also depend on R. In [11], we assumed an exponential behavior for these terms. Second, the superexchange mechanism can only be operative if the states of the bridge atom lie close in energy to the resonance since the couplings are inversely proportional to the energy difference. Finally, owing to electric dipole selection rules, only the channels with proper symmetries are enhanced in the presence of the bridge atom compared to the isolated case, i.e., there is no superexchange contribution if $\langle i|z|l\rangle$ and $\langle i|z|k\rangle$ are zero for symmetry reasons. For example, in the case of the NeHeNe trimer after $2s\sigma_g$ ionization only ICD channels leading to Ne^+HeNe^+ with at least one hole in $2p\sigma_u$ are enhanced.

The approximate expression obtained in Eq. (9) is used in the following to discuss the Fano-CI results.

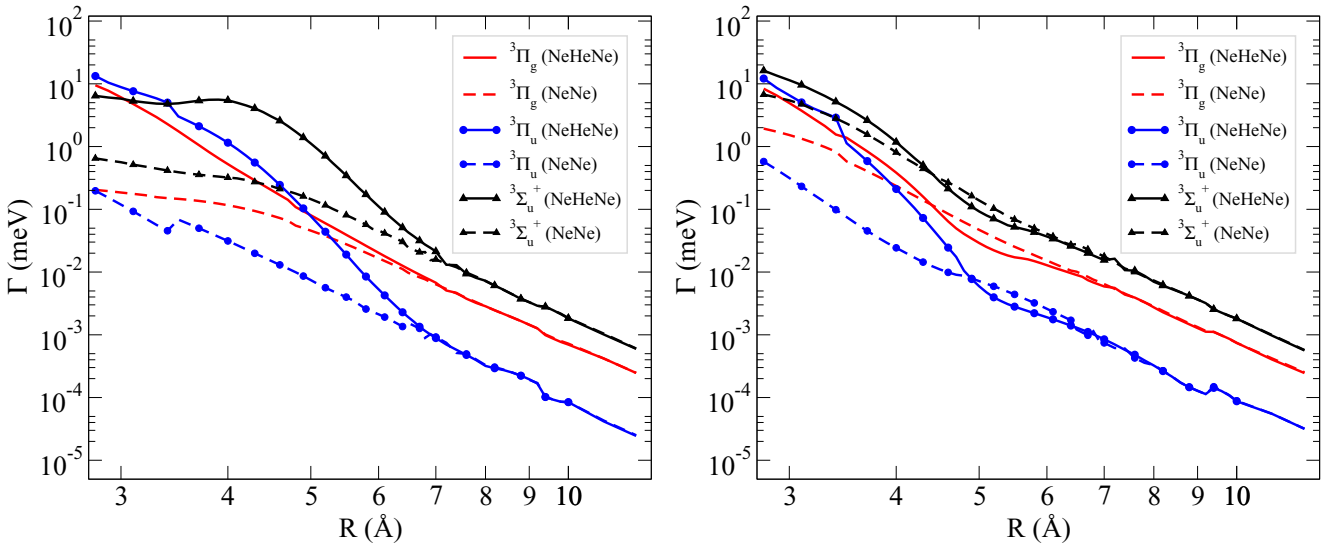

FIG. 3. Comparison between the partial decay widths of the $Ne^+(2s^{-1})\,^2\Sigma^+_{g,u}$ states in Ne_2 (dashed lines) and NeHeNe (full lines) to *triplet* final states. We show only the channels whose decay widths are enhanced as a result of the superexchange ICD: $^3\Pi_g$, $^3\Pi_u$, and $^3\Sigma^+_u$. Left panel: $Ne^+(2s^{-1})\,^2\Sigma^+_g$. Right panel: $Ne^+(2s^{-1})\,^2\Sigma^+_u$.

III. RESULTS AND DISCUSSION

A. Superexchange ICD in neon-helium-neon trimer

We first discuss the total ICD widths for linear NeHeNe trimer obtained with the Fano-CI method. Note that in [11] these widths were computed with the Fano-ADC method. Similar results are obtained here (see [13] for a comparison between the two methods). Figure 1 shows the total ICD widths for $^2\Sigma_g(2s^{-1})$ (left panel) and $^2\Sigma_u(2s^{-1})$ (right panel) states in NeHeNe compared to NeNe. We assume a linear geometry with helium located at the center of mass of the neon dimer. As in [11], a significant enhancement of the ICD widths is observed in the presence of the helium atom for R smaller than 6–7 Å.

After ICD, the doubly ionized trimer can be in one of the following twelve states (labeled as in the case of the isolated neon dimer): $^{1,3}\Delta_g$, $^{1,3}\Pi_g$, $^{1,3}\Pi_u$, $^1\Sigma^+_g$ ($\times 2$), $^1\Sigma^-_u$, $^3\Sigma^+_u$ ($\times 2$), and $^3\Sigma^-_g$. In Figs. 2 and 3, we report the partial widths of the states that are enhanced by the superexchange ICD mechanism. As seen in the figures, only ICD channels leading to $^{1,3}\Pi_g$, $^{1,3}\Pi_u$, one of the $^1\Sigma^+_g$ and $^3\Sigma^+_u$ states have enhanced widths in the presence of the bridge atom compared to the isolated case. This is in agreement with the symmetry reasoning obtained with the model presented in Sec. II B.

We note that for some distances a few partial ICD widths are smaller in the presence of the bridge atom than that in the isolated case. Such a decrease can be due to interference effects between the direct ICD and the superexchange ICD pathways, as well as some screening effects of the bridge species reducing thus the interaction between the two neon atoms. Further works are needed to investigate these effects.

B. Superexchange ICD in neon-helium-argon trimer

We now discuss the ICD process in the linear NeHeAr trimer. For the superexchange ICD mechanism, the main difference in this system compared to NeHeNe is the energies of the bridge states relative to the resonance energy. Assuming the energies of the bridge states are equal to those of He^- with two point charges at the position of the donor and acceptor atoms and that the energy of $2s$-ionized neon donor atom does not depend significantly on the nature of the acceptor atom, the difference between NeHeNe and NeHeAr is the ionization potential difference of Ne and Ar, which is about −5 eV. The bridge states lie therefore further away from the resonance energy in the case of NeHeAr. Assuming similar H_{Jf}, dipole and overlap terms in Eq. (9), it is expected that the superexchange mechanism is less effective in NeHeAr than in NeHeNe. In [13], we showed that the virtual states of the

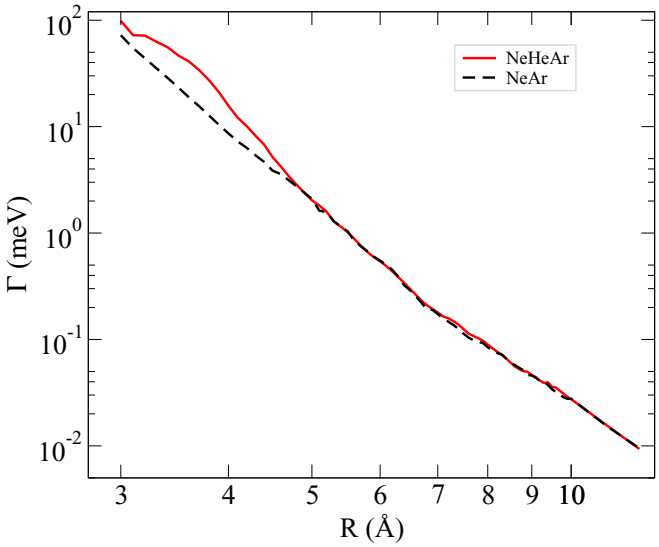

FIG. 4. Comparison between the total decay widths of the $Ne^+(2s^{-1})\,^2\Sigma^+$ states in NeAr (black dashed line) and NeHeAr (red full line).

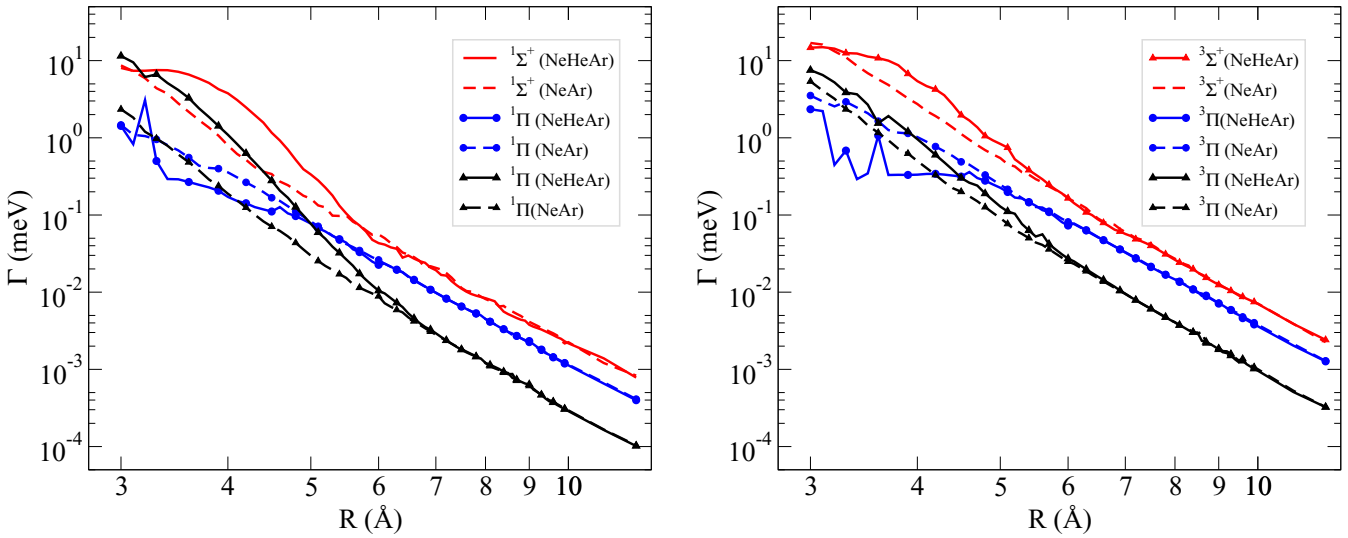

FIG. 5. Comparison between the partial decay widths of the $Ne^+(2s^{-1})\ ^2\Sigma^+$ state in NeAr and NeHeAr to *singlet* (left panel) and *triplet* (right panel) final states. We show only the channels whose decay widths are enhanced as a result of the superexchange ICD: $^1\Pi$, $^1\Sigma^+$ and $^3\Pi$, $^3\Sigma^+$.

bridge atom are between 3 eV and 16 eV below the resonance energy in the case of NeHeNe. A shift of −5 eV in Eq. (9) leads to a decrease of the superexchange ICD terms by a factor of between 0.35 and 0.6.

The total ICD widths in NeHeAr are shown in Fig. 4. As expected, the enhancement of the ICD widths in the presence of the helium atom is weaker and, moreover, starts to be operative at shorter interatomic distances in the case of NeHeAr compared to NeHeNe. Indeed, the superexchange mechanism is seen at distances below 5 Å in NeHeAr, while it starts below 7 Å for NeHeNe. Furthermore, the maximum enhancement is only of a factor of about 2 for the NeHeAr and of about 7 for NeHeNe. This decrease in the efficiency of the superexchange ICD mechanism in NeHeAr seen in the *ab initio* results agrees quantitatively with that predicted by our first-order perturbation-theory based model.

For completeness, we show the partial ICD widths in NeHeAr in Fig. 5. Among the final states, which are $^{1,3}\Delta$, $^{1,3}\Pi$ (×2), $^{1,3}\Sigma^+$ (×2), and $^{1,3}\Sigma^-$, only one of each $^{1,3}\Pi$ and $^{1,3}\Sigma^+$ are enhanced in agreement with the perturbation-theory based model. Note that, in the trimer case, the partial ICD widths for the Π states exhibit sharp peaks for some distances (e.g., at $R = 3.2$ Å in the left panel of Fig. 5), which are attributed to interferences between the two adiabatic Π states in each spin symmetry. Such interference effects will be discussed in a future publication.

IV. CONCLUSIONS

We have analyzed in detail the superexchange ICD mechanism in NeHeNe and NeHeAr. Total and partial ICD widths, computed with the Fano-CI method, are reported. It is shown that, owing to symmetry reasons, only some ICD channels are enhanced in the presence of helium as a bridge atom compared to isolated NeNe and NeAr dimers. Furthermore, due to the lower ionization potential of argon compared to neon, the energy of the bridge states of NeHeAr are further away from the resonance energy compared to NeHeNe. The superexchange contributions are therefore smaller and appear at shorter interatomic distances. A simple model based on first-order perturbation theory and a Hartree-Fock-like description of the states is reported. This model explains the observation made from the Fano-CI results and thus provides insight into the superexchange ICD mechanism. NeHeNe and NeHeAr have been employed in this work because they allow an accurate theoretical description. However, related phenomena are known in resonance energy transfer within molecular aggregates (see, for example, Ref. [23]) and excitation transfer along covalent bonds in large molecules [24], which suggest that the superexchange ICD mechanism is more general. Further experimental and theoretical works on atomic and molecular clusters with different bridge systems are needed to unravel the full importance of this mechanism.

ACKNOWLEDGMENTS

This project has received funding from the Research Executive Agency (REA) under the European Union's Horizon 2020 research and innovation programme Grant agreement No. 705515. P.K. and P.V. acknowledge financial support by the Czech Science Foundation (Project GAČR No. 17-10866S).

[1] L. S. Cederbaum, J. Zobeley, and F. Tarantelli, Phys. Rev. Lett. **79**, 4778 (1997).

[2] S. Marburger, O. Kugeler, U. Hergenhahn, and T. Möller, Phys. Rev. Lett. **90**, 203401 (2003).

[3] T. Jahnke, A. Czasch, M. S. Schöffler, S. Schössler, A. Knapp, M. Käsz, J. Titze, C. Wimmer, K. Kreidi, R. E. Grisenti, A. Staudte, O. Jagutzki, U. Hergenhahn, H. Schmidt-Böcking, and R. Dörner, Phys. Rev. Lett. **93**, 163401 (2004).

[4] R. Santra, J. Zobeley, L. S. Cederbaum, and N. Moiseyev, Phys. Rev. Lett. **85**, 4490 (2000).
[5] K. Schnorr, A. Senftleben, M. Kurka, A. Rudenko, L. Foucar, G. Schmid, A. Broska, T. Pfeifer, K. Meyer, D. Anielski, R. Boll, D. Rolles, M. Kübel, M. F. Kling, Y. H. Jiang, S. Mondal, T. Tachibana, K. Ueda, T. Marchenko, M. Simon, G. Brenner, R. Treusch, S. Scheit, V. Averbukh, J. Ullrich, C. D. Schröter, and R. Moshammer, Phys. Rev. Lett. **111**, 093402 (2013).
[6] V. Averbukh, P. V. Demekhin, P. Kolorenč, S. Scheit, S. D. Stoychev, A. I. Kuleff, Y.-C. Chiang, K. Gokhberg, S. Kopelke, N. Sisourat, and L. S. Cederbaum, J. Electron. Spectrosc. Relat. Phenom. **183**, 36 (2011).
[7] U. Hergenhahn, J. Electron. Spectrosc. Relat. Phenom. **184**, 78 (2011).
[8] T. Jahnke, J. Phys. B: At., Mol., Opt. Phys. **48**, 082001 (2015).
[9] See http://www.pci.uni-heidelberg.de/tc/usr/icd/ICD.refbase.html for the complete list of ICD papers.
[10] V. Averbukh, I. B. Müller, and L. S. Cederbaum, Phys. Rev. Lett. **93**, 263002 (2004).
[11] T. Miteva, S. Kazandjian, P. Kolorenč, P. Votavová, and N. Sisourat, Phys. Rev. Lett. **119**, 083403 (2017).
[12] R. Bennett, P. Votavová, P. Kolorenč, T. Miteva, N. Sisourat, and S. Y. Buhmann, Phys. Rev. Lett. **122**, 153401 (2019).
[13] T. Miteva, S. Kazandjian, and N. Sisourat, Chem. Phys. **482**, 208 (2017).
[14] U. Fano, Phys. Rev. **124**, 1866 (1961).
[15] G. Howat, T. Åberg, and O. Goscinski, J. Phys. B: At., Mol., Opt. Phys. **11**, 1575 (1978).
[16] A. U. Hazi, in *Electron-Molecule and Photon-Molecule Collisions*, edited by T. Rescigno, V. McKoy, and B. Schneider (Plenum Press, New York, London, 1979).
[17] P. W. Langhoff, in *Electron-Molecule and Photon-Molecule Collisions*, edited by T. Rescigno, V. McKoy, and B. Schneider (Plenum Press, New York, London, 1979).
[18] F. Müller-Plathe and G. H. F. Diercksen, Phys. Rev. A **40**, 696 (1989).
[19] V. Averbukh and L. S. Cederbaum, J. Chem. Phys. **123**, 204107 (2005).
[20] T. H. Dunning, J. Chem. Phys. **90**, 1007 (1989).
[21] K. Kaufmann, W. Baumeister, and M. Jungen, J. Phys. B: At., Mol., Opt. Phys. **22**, 2223 (1989).
[22] R. Santra and L. S. Cederbaum, Phys. Rep. **368**, 1 (2002).
[23] A. Salam, J. Chem. Phys. **136**, 014509 (2012).
[24] A. I. Kuleff, Chem. Phys. **482**, 216 (2017).